Supporting Information for

Biomimetic calcium-inactivated ion/molecular channel

Minmin Li,[ab] Yuchen Cao,[bc] Xin Zhang,[b] Dongdong Wang[b], Shengxu Qian[b], Guodong Li[b], Fushen Zhang[b], Yuting Xiong,*[ab] and Guangyan Qing*[b]

[a] Jiangxi Province Key Laboratory of Polymer Micro/Nano Manufacturing and Devices, East China University of Technology, 418 Guanglan Avenue, Nanchang 330013, China.
E-mail: xiongyt@dicp.ac.cn.
[b] CAS Key Laboratory of Separation Science for Analytical Chemistry, Dalian Institute of Chemical Physics, Chinese Academy of Sciences, 457 Zhongshan Road, Dalian 116023, China.
E-mail: qinggy@dicp.ac.cn.
[c] Zhang Dayu School of Chemistry, Dalian University of Technology, Dalian 116024, China.

Table of contents

1. Materials and instruments

Polyethylene terephthalate (PET) foils of 12 μm thickness and 30 mm diameter were irradiated at the linear accelerator UNILAC (GSI, Darmstadt) with swift heavy ions having an energy of 11.4 MeV per nucleon with one ion track and with 10^6 ions·cm^{-2} ion tracks in the center domain. *N*-hydroxysuccinimide (NHS) was purchased from Alfa Aesar (China) Chemical Co., Ltd. *N*-acetyl-L-arginine, 1-(3-dimethylaminopropyl)-3-ethylcarbodiimide hydrochloride (EDC) was purchased from TCI Shanghai (China). Various metal chloride (KCl, NaCl, $CaCl_2$, $MgCl_2$, $AlCl_3$, LiCl, $BaCl_2$, $ZnCl_2$, $CuCl_2$) used in the work were purchased from Sigma-Aldrich Corp. (China), Beijing Innochem Co., Ltd. (China), or Sinopharm Chemical Reagent Co., Ltd. (China). A di-phosphorylated peptides D***p***S***p***SEEKC (abbreviated as PP) was purchased from China-Peptides Corp. (Shanghai, China) with high purity (> 95%). Deuterated dimethylsulfoxide (DMSO-d_6) and deuterium oxide (D_2O) were purchased from Beijing Innochem Co., Ltd. (China). Other general solvents and reagents were purchased from Sinopharm Chemical Reagent Co., Ltd. (China). The water used in this study was purified by Milli-Q system (18.2 MΩ·cm).

All NMR spectra were recorded on Bruker Avance III 400M NMR spectrometer (Bruker Corp., Germany). Scanning electron microscope (SEM) images were obtained on a Hitachi FlexSEM1000. X-ray photoelectron spectroscopy (XPS) was obtained with a ESCALAB250xi (Thermo Fisher Scienti.fic, US). Surface contact angle data were obtained from KRUSS DSA 100 (KRÜSS GmbH, Germany). All current-voltage curves were measured by a Keithley 6487 picoammeter (Tektronix Inc., US). Surface potential was measured with Bruker Dimension Icon atomic force microscope (AFM) in the mode of Kelvin Probe Force Microscope (KPFM). Isothermal titration microcalorimetry (ITC) experiment was conducted on a MicroCal ITC 200 system (Malvern Panalytical Ltd., UK). Fluorescent spectra were obtained by using a Perkin-Elmer FL-6500 fluorescence spectrometer. UV-Vis spectra were obtained by using a LAMBDA 365 UV-Vis spectrophotometer.

2 Preparation of PET nanochannel.

The single conical nanochannel was fabricated according to the method developed by Apel et al. and some modifications.[1] First, both side of a single ion-irradiated PET foil was irradiated by UV light for 30 minutes, respectively. Then the PET foil was mounted between two tailor-made Teflon modules in a stainless-steel holding apparatus, in which the foil serves as an isolation valve (Scheme S2). The chamber of one Teflon module was filled with the etching solution (9 M NaOH), the other was filled with the stopping solution (1M HCOOH + 1M KCl). The etching was performed at around 60 °C. During the etching process, the potential of 1 V was applied to be used to monitor the etching process, where the transmembrane ionic current begins to increase as soon as the nanochannel opened. Then, the etching process was stopped by replacing the etching solution with stopping solution when the ionic current reached a certain desired value. Finally, the PET foil was taken out and washed with ultrapure water, and then immersed in water to remove residual salts.

Similarly, the multiple nanochannel PET membrane based on a PET foil with 10^6 ion tracks per square centimeter was obtained under the equal etching condition. In addition, an ion-track-free PET foil was also etched by the 9 M NaOH with the same etching time to use to simulate the PET nanochannel inner surface.

The morphology and pore diameter (d_{base}) of the large opening (base side of the conical nanochannel) of the obtained conical nanochannel was characterized by SEM. The small opening (tip side of the conical nanochannel) and the section of the conical nanochannel was seen on the PET membrane with multiple conical nanochannels.

3. Modification of PET nanochannel with the phosphopeptide.

Carboxyl groups generated on the nanochannel inner wall as a gift of the chemical etching process provide the abundant active groups to further modification.[2] Specifically, as shown in Scheme S1, the PET nanochannel was immersed in EDC/NHS (5mL, 75 mg EDC and 45 mg NHS) aqueous solution for 2h to activate the surface carboxyl groups. The formed amine-reactive ester intermediate was condensed with ethylenediamine (EDA) solution (10mM) overnight. After that, the PET foil was washed with lots of water. Then, the PET foil with EDA was immersed into PP (10 mM) solution with EDC/NHS (5mL, 75 mg EDC, 45 mg NHS, and 48 mg PP) for 24 hours, where one of the carboxyl groups of PP condensed with EAD amino group once the carboxyl group was activated by EDC/NHS. Subsequently, PP modified PET nanochannel (abbreviated as PP nanochannel) foil was washed with lots of water to remove residual chemicals, and then immersed in water.

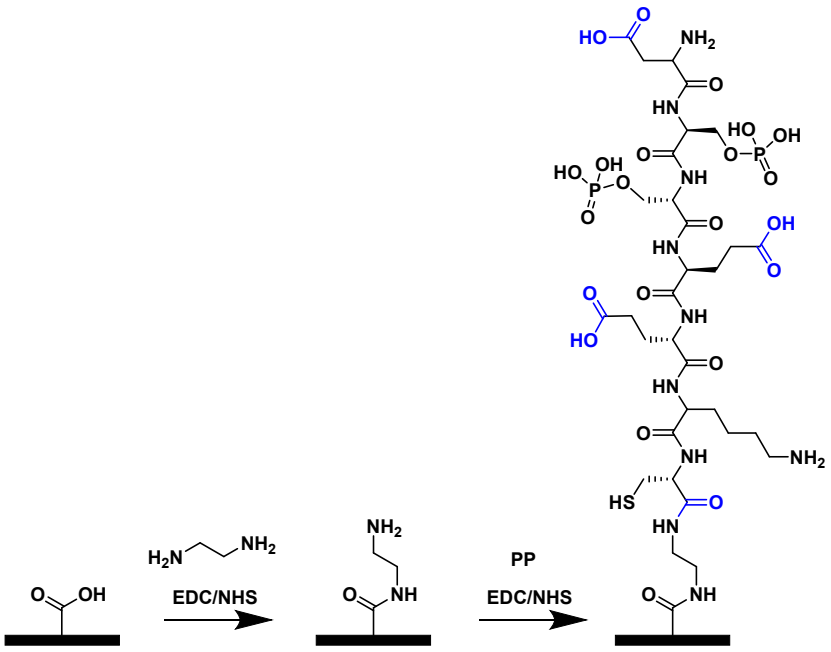

Scheme S1 Preparation of the PP modified nanochannel by two step EDC/NHS coupling reactions mediated by ethylenediamine. The PP molecule was fixed onto nanochannel surface by one of its carboxyl groups (blue color in the structure).

4. Ionic current measurement of nanochannel

Firstly, the PP nanochannel membrane was mounted between two tailor-made Teflon modules in a stainless-steel holding apparatus. Both chambers of two Teflon modules were filled with 0.1M KCl aqueous solution as the electrolyte solution. The prepared KCl solution shows a pH of 5~6. Thus, we adjusted the pH of KCl solution to 7.5 with 1M NaOH in order to assure the neutral electrolyte. The transmembrane ion current was measured by using a Keithley 6487 picoammeter. Ag/AgCl electrodes were used to apply a transmembrane potential across the membrane (Scheme S2A). The transmembrane potential was a sweep voltage varied from −2 V to +2 V with a step voltage of 0.2 V and a step time of 1 s. The ionic current obtained from the injection of 0.1M KCl solution was assigned as the initial current value (i.e., the blank ion conductance). Then, various cation solutions with different concentrations were prepared based on this neutral 0.1M KCl aqueous solution. Prior to each test, a solution was injected into both chambers, and the corresponding ionic current was recorded after an incubation process of 20~30 minutes. Each ionic measurement was repeated for 3 times to obtain the average current value along with the standard deviation.

In addition, to explore the response of Na^+ and Li^+ flow passing through PP nanochannel toward Ca^{2+}, 0.1M NaCl and LiCl solution (pH 7.5) were prepared. A series of Ca^{2+} solutions with different concentrations were prepared based on the 0.1M NaCl and LiCl solution, respectively, and used to measure the ionic current of PP nanochannel.

To test the reversibility and stability of the response of PP nanochannel to Ca^{2+}, we chose EDTA (i.e., EDTA-2Na) solution to treat the Ca^{2+}-treated PP nanochannel. As shown in Scheme S2B, the two chambers of the electrochemical apparatus were refilled with the EDTA-2Na solution (1 mM). The processing time was maintained for half an hour or so. Then the EDTA-2Na solution were exchanged to water to wash the PP nanochannel (Scheme S2C). After this process, we further test the ion current of PP nanochannel by refilling the two chambers of the electrochemical apparatus with 0.1M KCl aqueous solution. Thereupon, a cycle of alternately treating PP nanochannel with Ca^{2+} and EDTA was completed.

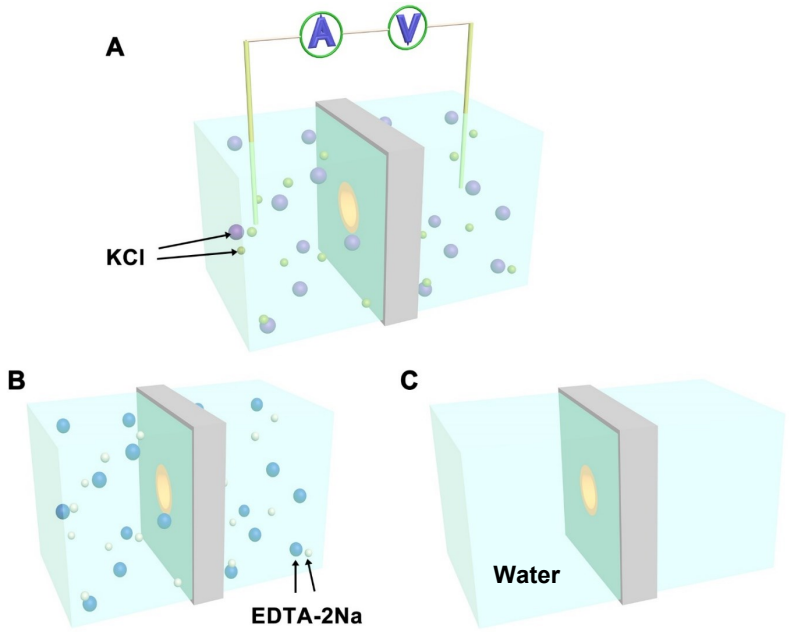

Scheme S2 (A) Schematic illustrating the ionic current measurement apparatus mounted with PP nanochannel membrane. Purple ball denotes the potassium ion (K^+), and green ball denotes the chloride ion (Cl^-). (B) Schematic illustrating the EDTA treatment process for the Ca^{2+} treated PP nanochannel. (C) Schematic illustrating the water washing treatment of PP nanochannel.

5. ITC experiment.

ITC analysis was employed to investigate the binding details of PP molecule with calcium ion (Ca^{2+}). The experiment was performed by Microcal ITC 200 at 25 ºC. PP (2 mM) and $CaCl_2$ (20.0 mM) were dissolved in the fresh-prepared Milli-Q water sufficiently to prepare the work solutions. The $CaCl_2$ solution was loaded into the syringe and titrated into the calorimetric cell containing the PP solution. The reference cell was filled with the fresh-prepared Milli-Q water. The titration sequence consisted of a single 0.4 μl injection followed by a series of 2 μL solution, with a time interval of 180s between injections to ensure that the thermal power returns to the baseline before the next injection. The stirring speed was 1000 rpm.

The exothermic heat values were analyzed using Origin7.0 software package (OriginLab, Northampton, MA). PP molecule has multiple acidic negatively charged groups (two phosphoryl groups and four carboxyl groups) that are available to coordinate Ca^{2+}. Thus, we used the sequential binding model to fit the data to yield the equilibrium association constant (K_a) and other thermodynamic parameters.

6. Surface contact angle measurement

As shown in Scheme S3, an ion-track-free PET foil was etched by the 9 M NaOH with the same etching time and etching process to use to simulate the PET nanochannel inner surface. After etching, the PET foil was immerged in Milli-Q water overnight. The further modification on PET foil with PP adopted the same method with the nanopore. The PP modified PET foil was washed with water, then dried with N_2.

Contact angles measurement were carried out at ambient temperature. In each measurement, an about 2 μL droplet of water was dispensed onto the sample surface. The average contact angel value was obtained at five different positions of the same membrane. In addition, the PP modified PET foil was immersed in $CaCl_2$ aqueous solution (10 μM) (pH 7.5) for 20 minutes. Then Ca^{2+}-treated PET foil was rinsed with water and dried with N_2. In the same procedure, contact angle was measured.

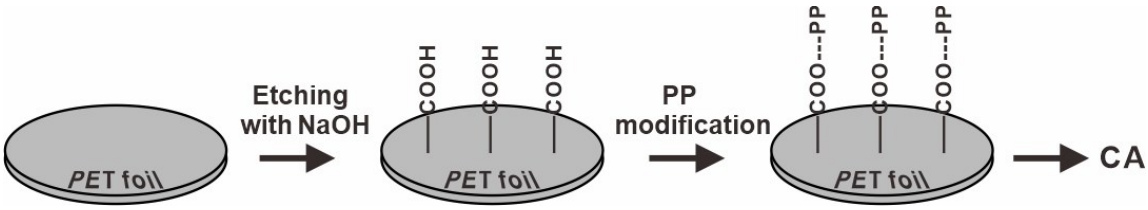

Scheme S3 The modification of ion-track (or ion nanochannel)-free PET foil with PP for purpose of measuring the surface contact angle (CA) as the analogue of PP nanochannel inner surface.

7. Electroosmotic flow (EOF) measurement and charge density calculation

Electroosmotic flow (EOF) is an electrokinetic phenomenon that occurs when an ion flow passed through a channel that contains excess surface charge.[3] Here, EOF was driven through PET nanochannel membrane by mounting the membrane between two electrolyte solutions and applying a bias voltage in two electrolyte solutions to produce constant ionic current through the nanochannel. Generally, EOF rate was obtained by measuring the flux of a neutral probe molecule (i.e., phenol) through the nanochannel. In this work, the prepared PP nanochannel has excess negative charges on inner surface. Thus, EOF is in the direction of cation ion migration across the channel. Considering the shape of asymmetric cone of the nanochannel, EOF direction along with cation ion migration is from the cone tip (small opening of nanochannel) to the base (large opening of nanochannel).

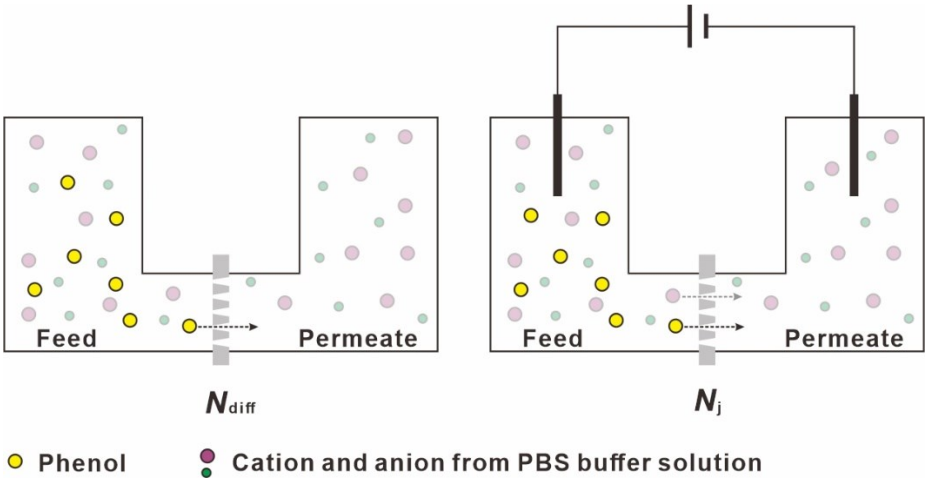

Scheme S4 Schematic illustrating the EOF measurement.

Here, we choose the PP modified PET foil with multiple nanochannels (the nanochannel density is 10^6 per square centimeter) to conduct the EOF measurement in order to measure the phenol flux more accurately. Firstly, the nanochannel membrane was clamped between two tailor-made Teflon modules in a stainless-steel holding apparatus, as shown in Scheme S4. In this apparatus, the nanochannel membrane exposes a 0.2-cm^2 portion to the electrolyte solution. The feed chamber was filled with 10 mM phosphate buffer (pH 7.5) containing 10 mM phenol. The permeate chamber was filled only with buffer solution. The EOF was driven from feed to permeate by using a Pt electrode in each chamber solution to apply a bias voltage of 2 V. The anode was in the Feed solution in EOF experiments.

The EOF velocity was determined by measuring the transport of phenol across the nanochannels and into the permeate solution. This was accomplished by periodically detecting the phenol in the

permeate solution with a UV/Vis detector and making plots of phenol molar (absorbance in UV/Vis spectrum) *vs* time. The corresponding slope from fitting these plots is proportional to the phenol flux through the nanochannel. When phenol transport is assisted by EOF, the total flux, N_j, has both diffusive and electroosmotic contributions (Scheme S3, right panel). While, the diffusive flux, N_{diff}, was obtained independently by doing an analogous experiment in the absence of current (Scheme S3, left panel). Thus, N_j and N_{diff} were then used to calculate the enhancement factor E

$$E = \frac{N_j}{N_{diff}} \quad (1)$$

Then the obtained enhancement factor E was used to calculate the Peclet number, Pe, using

$$E = \frac{Pe}{1 - e^{-Pe}} \quad (2)$$

The electroosmotic velocity, v_{eof}, was obtained via

$$v_{eof} = \frac{Pe \times D}{L} \quad (3)$$

where L is the membrane thickness 12 μm and D is the diffusion coefficient for phenol, 8.9×10^{-6} $cm^2 \cdot S^{-1}$.

In addition, the Helmholtz-Smoluchowski equation describes the relationship between the electroosmotic velocity with solution resistivity, ρ, and the applied current density J_{app}

$$v_{eof} = -\varepsilon \times \zeta \times J_{app} \times \frac{\rho}{\eta} \quad (4)$$

where ε and η are the permittivity and viscosity of the solution (here, the permittivity and viscosity of water are 6.95×10^{-10} $C^2 \cdot J^{-1} \cdot m^{-1}$ and 0.893×10^{-3} $N \cdot S \cdot m^{-2}$, respectively), J_{app} is the constant applied current density (ratio of the applied current with the area of all nanochannel opening), ρ is the solution resistivity (2.23×10^3 Ω·m), and ζ is the zeta potential of the pore wall.

Furthermore, the obtained ζ was used to calculate the surface charge density via

$$\zeta = \frac{\sigma \times \kappa^{-1}}{\varepsilon} \quad (5)$$

and

$$\kappa^{-1} = \frac{9.61 \times 10^{-9}}{\sqrt{z^2 \times C}} \quad (6)$$

where κ^{-1} is the effective thickness of the electrical double layer, z is the charge of the permeate ion (i.e., the valence state of the diffused counter ion, Na^+ from PBS buffer), C the concentration of diffusion ion (10 mM).

8. Surface potential measurement

Kelvin probe force microscopy (KPFM) is a complementary technique to the AFM and is a sensitive method to detect the local electrostatic potential. It is increasingly used in biophysics to investigate the interaction of biomolecules and visualize the surface potential distribution of biomolecules in air.[4] The basic principle of KPFM imaging is to measure the electric field force acting on a AFM cantilever tip due to electrical charges on the surface of a nanoscale object.

A PFQNE-AL probe, i.e., sharp nitride lever probe, that ideally suited for Peak Force Quantitative Nano-Electric measurement was chose here to perform surface potential measurement. Set the Interleave gains: Input I gain = 1, Input P gain = 5. Amplitude setpoint was set to 240 mV. Drive frequency and amplitude were set to 260 kHz and 500 mV, respectively. In the Interleave panel, the Interleave mode was set to LIFT. And Lift Scan Height was set to 100 nm.

PP modified ion-track-free PET foil was chosen as the analogue of PP nanochannel inner wall to study the surface potential. Firstly, the PP modified PET foil was dried with N_2, and then fixed onto the sample holder to measure the surface potential. After being immersed in $CaCl_2$ aqueous solution (10 μM) (pH 7.5) for 20 minutes and a washing with water and drying process with N_2, the surface potential of the Ca^{2+}-bound PP modified PET foil was measured.

The obtained images were processed with Nasoscope Analysis v1.8.

9. Molecular transport experiment

It has been acknowledged that excessive negative charges in PP nanochannel inner wall facilitates the transport of positive ions or molecules. Here, the transport of positively charged molecule through PP nanochannel and its response to Ca^{2+} were investigated. First, rhodamine b, a positively charged fluorophore, was chose as the probe molecule. Then, PP modified PET foil with multiple nanochannels (the nanochannel density is 10^6 per square centimeter) was employed to conduct molecular transport experiment. As shown in Scheme S5, the feed chamber was filled with 10 mM Rhodamine B solution (the solution pH was adjusted to 7.2 with 1M NaOH). The permeate chamber was filled with milli-q water. The transport of Rhodamine B across PP nanochannel was detected by periodically monitoring the Rhodamine B molecule in the permeate solution with a fluorescence spectrometer.

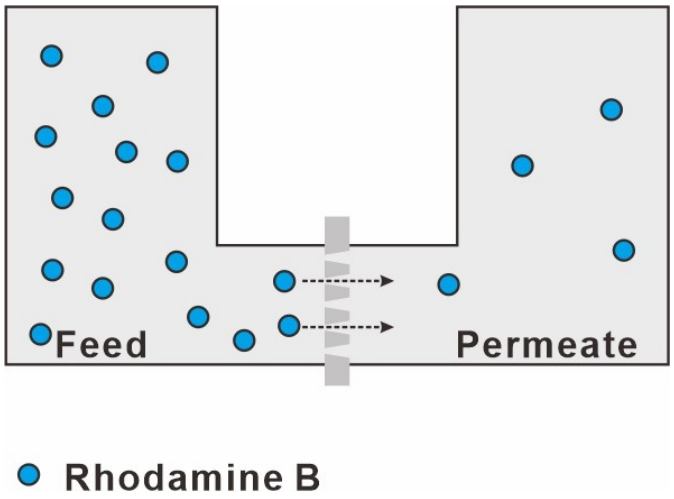

Scheme S5 Schematic illustrating the molecular transport experiment.

10. Supplementary Figures and Table

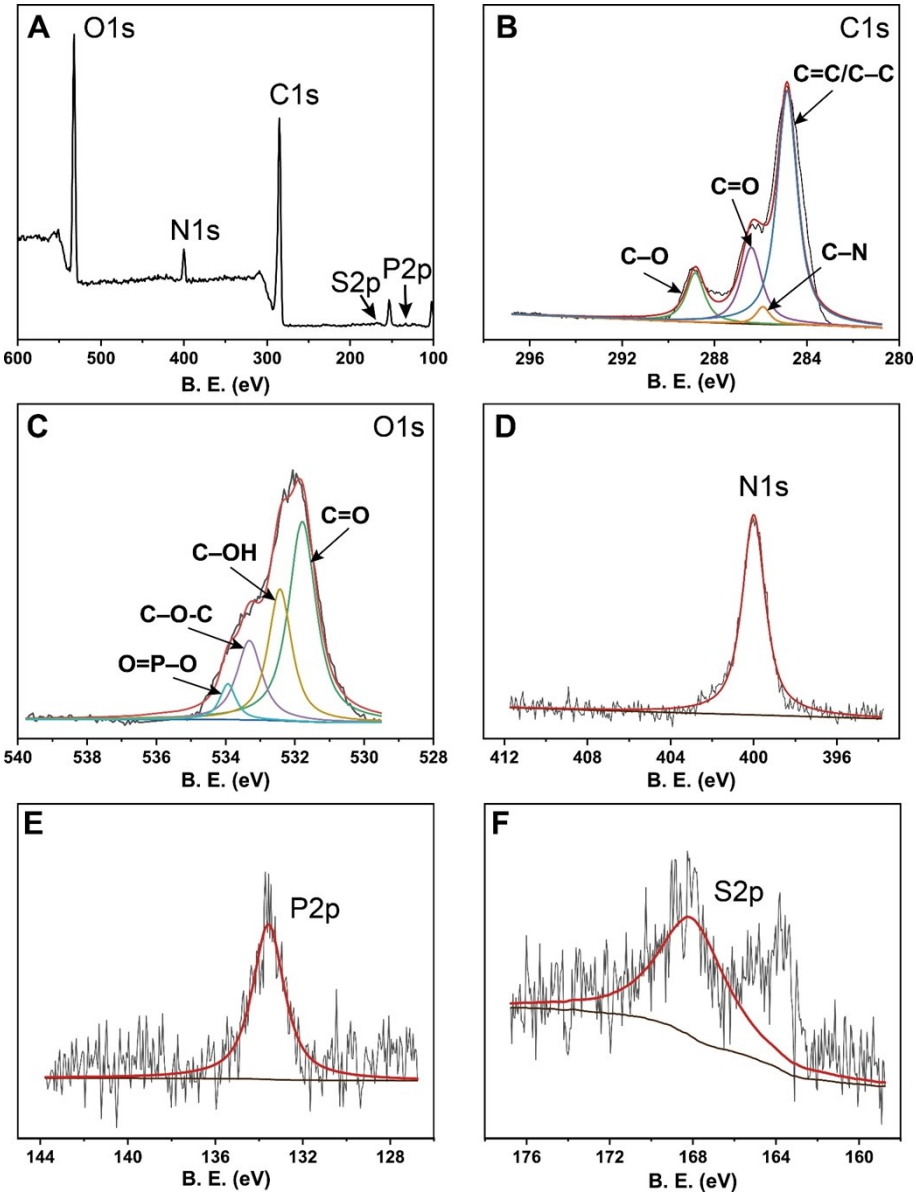

Fig. S1 XPS wide-scan spectrum (A) and C1s (B), O1s (C), N1s (D), P2p (E), and S2p (F) core-level spectra (b) of the PP modified nanochannel membrane.

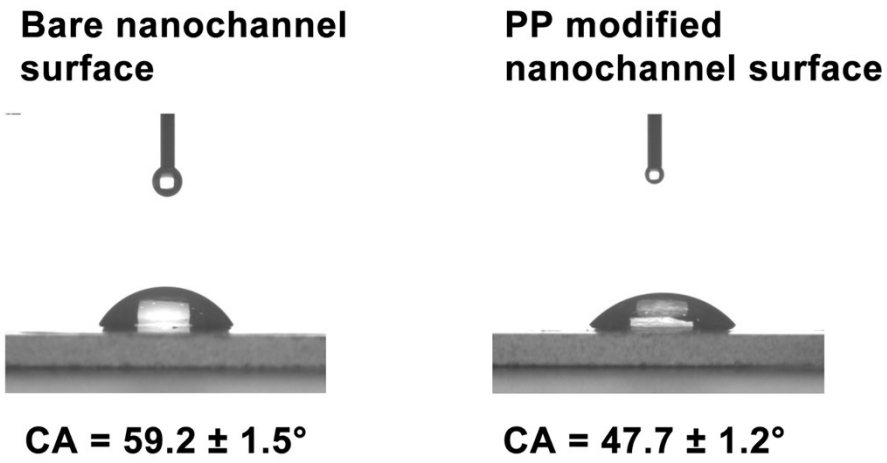

Fig. S2 Surface water contact angle (CA) change of the chemically etched PET foil (A) before and (B) after being modified with PP molecule. The wettability of chemically etched PET foil surface changed more hydrophilic after the modification of highly hydrophilic PP molecule.

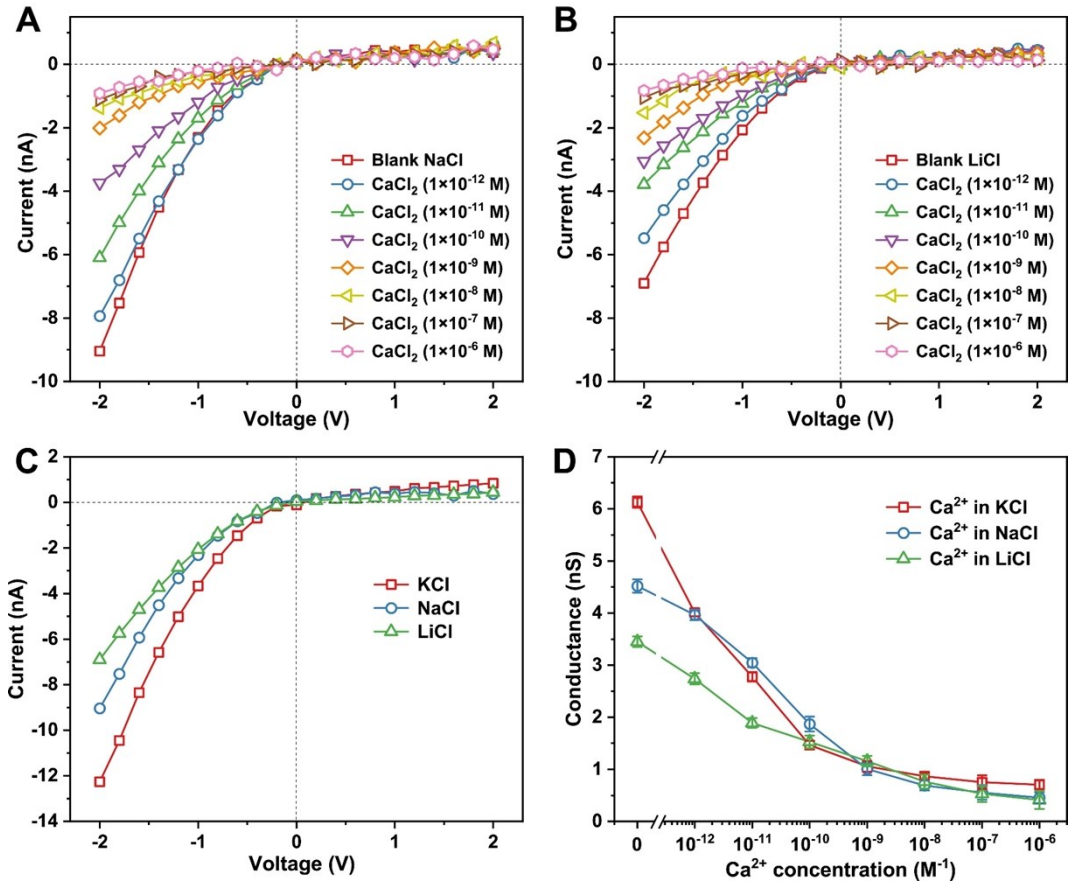

Fig. S3 (A, B) *I–V* plots of PP nanochannel upon addition of different concentration of Ca^{2+} solution in 0.1 M NaCl (A) and LiCl (B). (C) Comparison of *I–V* plots of PP nanochannel upon addition of different blank electrolytes. (D) Ca^{2+} concentration-dependent conductance (at –2V) changes of PP nanochannel toward in different electrolytes.

As shown in Fig. S3C and Fig. 1D in main text, the bare PP nanochannel displays different *I–V* plots toward KCl, NaCl, and LiCl electrolyte solutions with the same concentration. Here, the observed ion rectification effect results from the contribution of the cation in electrolyte for PP nanochannel that features a negatively charged inner surface. Thus, the difference in ion current toward KCl, NaCl, and LiCl is contributed by the difference among K^+, Na^+ and Li^+. The ionic current (which refers to the absolute value of ionic current at –2V, similarly hereinafter) (or the ion conductance) decreases gradually from KCl, to NaCl and to LiCl under the same concentration, which is consistent with the reported results.[5] The size order of hydrated ionic radius of these cations is $K^+ < Na^+ < Li^+$.[6] The smaller hydrated ionic radius can produce the higher ion mobility in solution, thus the higher ion conductance, and vice versa. Despite the difference of ion conductance, Ca^{2+}-induced inactivation effect of PP nanochannel for the K^+, Na^+ or Li^+ flow remains remarkable.

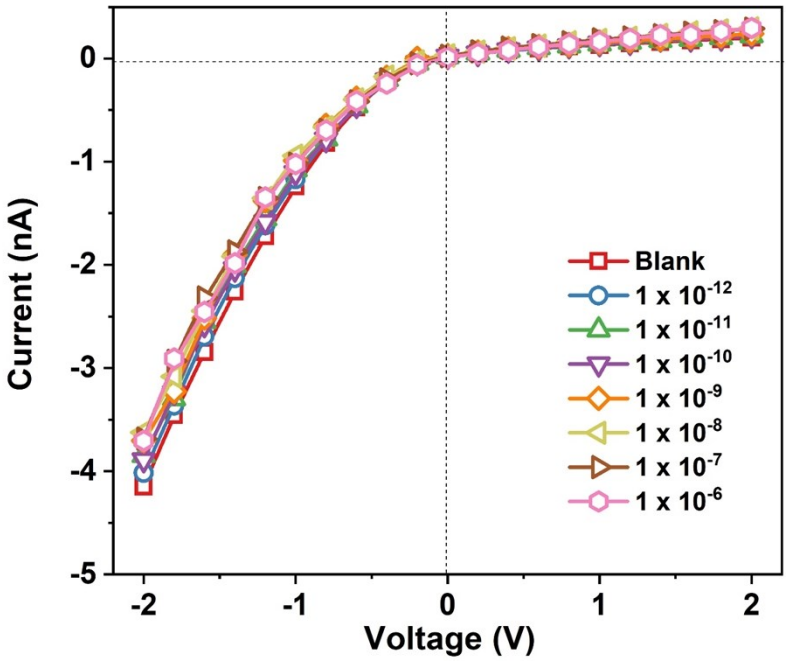

Fig. S4 *I–V* curves of the bare PET nanochannel upon addition of different concentration of Ca^{2+} solution prepared based on 0.1 M KCl.

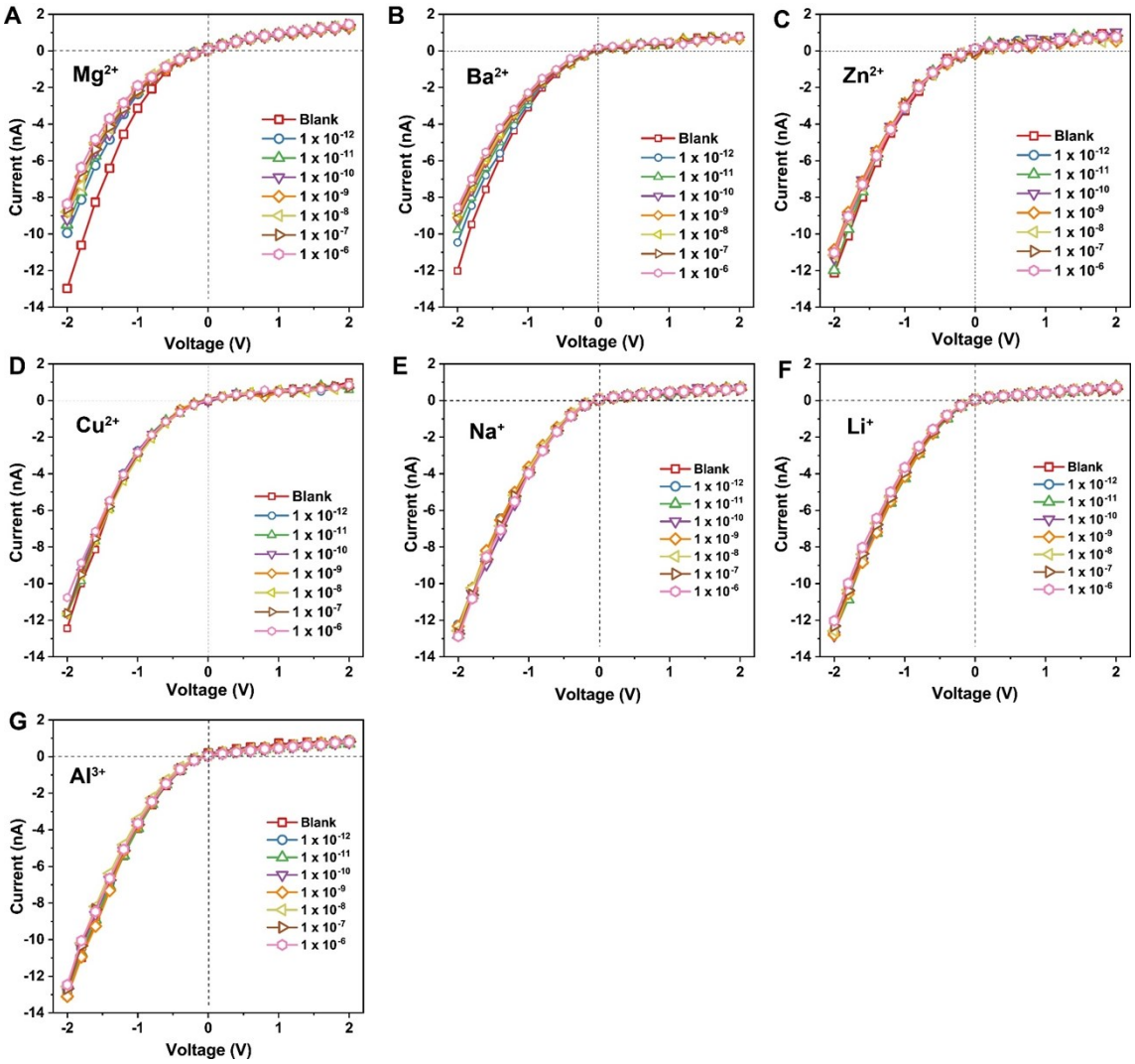

Fig. S5 *I–V* curves of PP nanochannel upon addition of different concentration of Mg^{2+} (A), Ba^{2+} (B), Zn^{2+} (C), Cu^{2+} (D), Na^{+} (E), Li^{+} (F), Al^{3+} (G) solution prepared based on 0.1 M KCl.

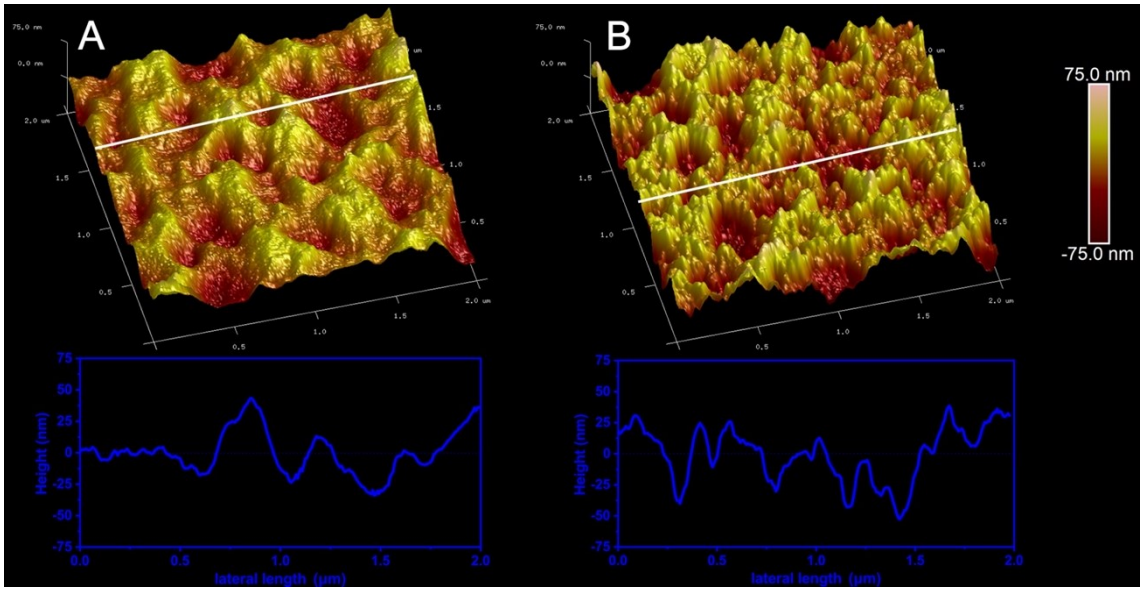

Fig. S6 The AFM height image and the corresponding section profile along with the white line of PP modified PET foil surface (A) before and (B) after being treated with Ca^{2+}. As shown in this figure, PP modified PET foil surface after Ca^{2+} treatment appears to be more rough versus the orignial surface

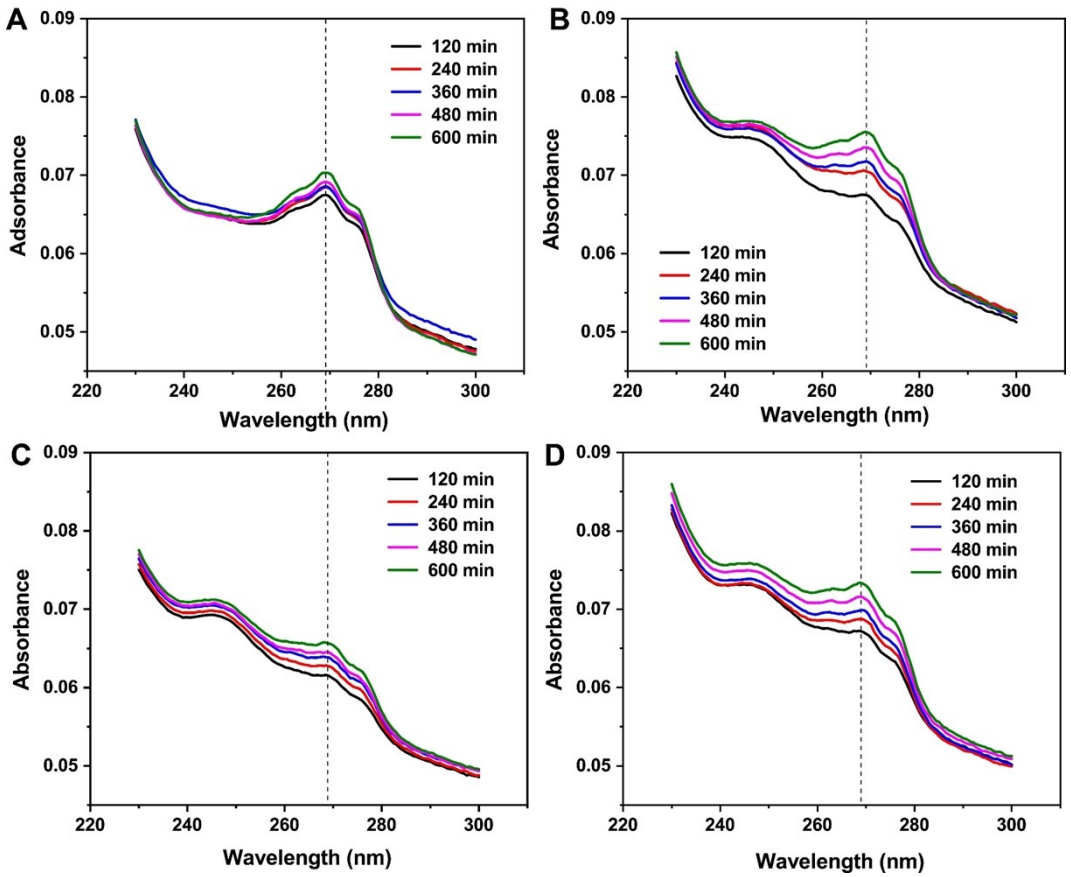

Fig. S7 Time-dependent absorbance increase of phenol transport from Feed solution to permeate across PP nanochannel (A) without and (B) with an external electric field, and Ca^{2+}-bound PP nanochannel (C) without and (D) with an external electric field.

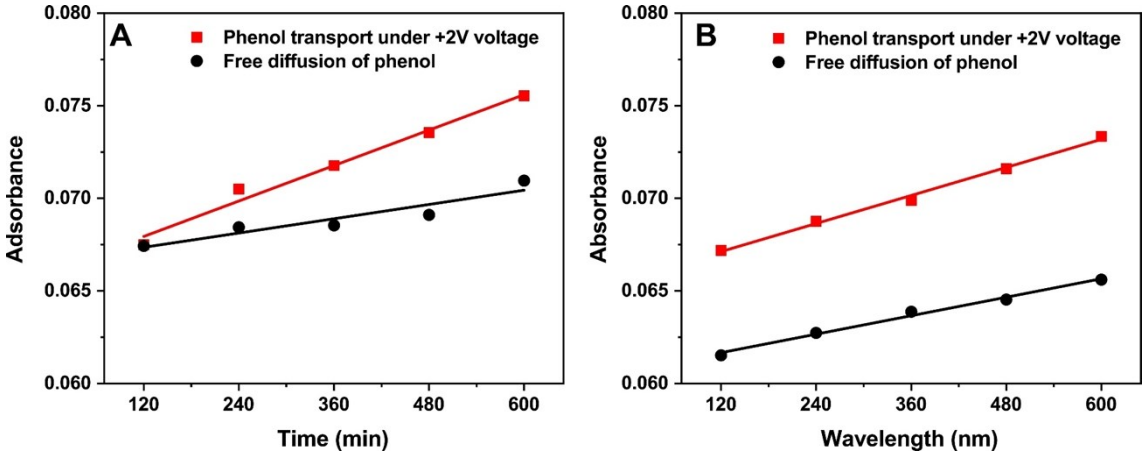

Fig. S8 Absorbance-time plots of phenol transport and the corresponding linear fitting.

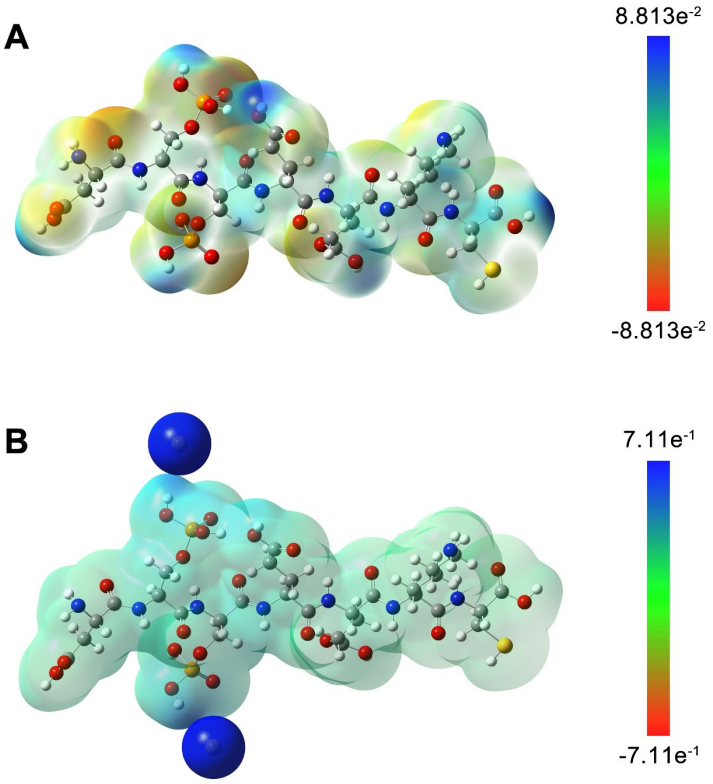

Fig. S9 The change in surface electrostatic potential distribution of PP upon binding with Ca^{2+}. Negative, neutral and positive electrostatic potentials are displayed in red, green and blue, respectively. The binding model involving two Ca^{2+} and two phosphoryl groups was taken for example. The electrostatic surface potential was carried out through density-functional-theory(DFT) method in the Gaussian 09 program by B3LYP, in combination with the triple-ζ valence quality with one set of polarization functions (TZVP).

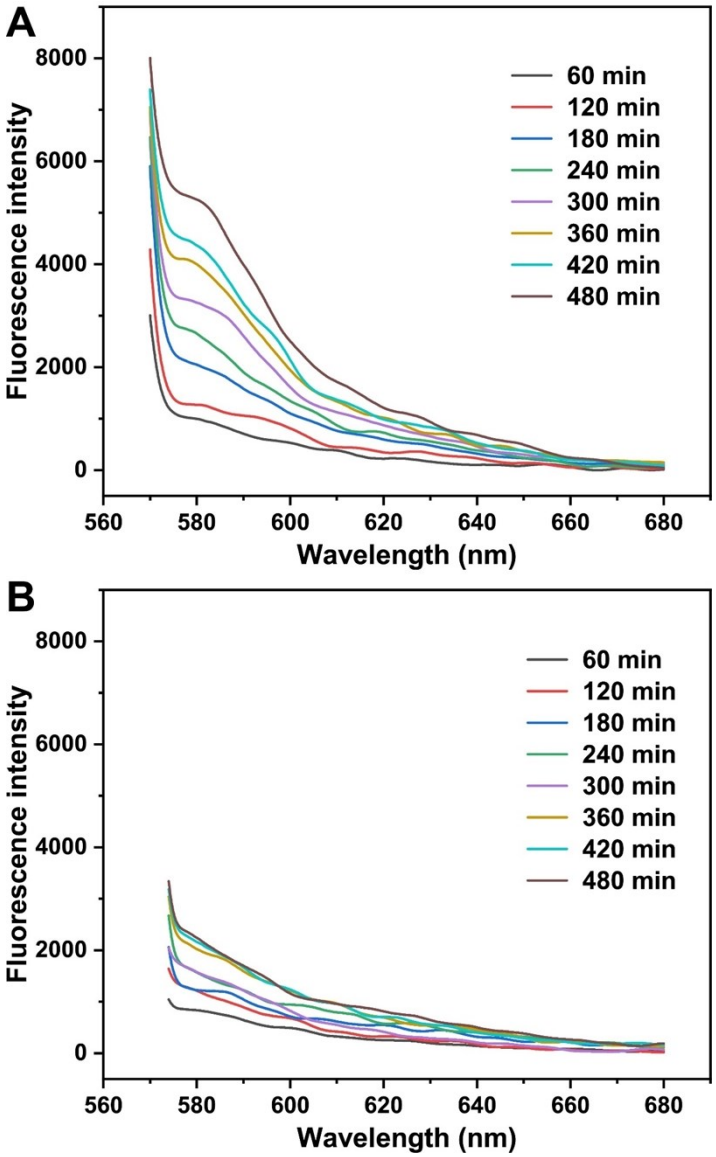

Fig. S10 Time-dependent fluorescence spectra of Rhodamine B passing through PP nanochannel (A) and Ca^{2+}-bound PP nanochannel (B).

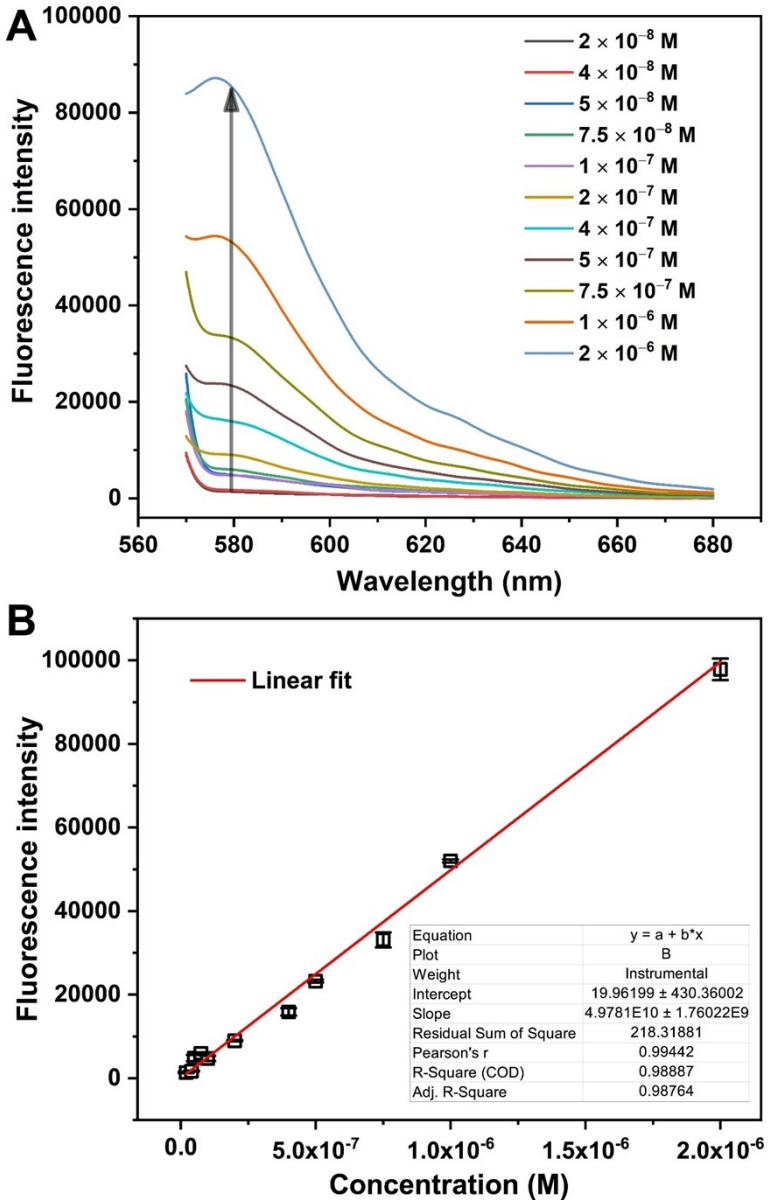

Fig. S11 Concentration-dependent fluorescence spectra of Rhodamine B solution (A) and the obtained fluorescence calculation curve (B).

Table S1 Association constant (K_a) values and thermodynamic parameters on the interaction of PP with Ca^{2+} obtained from ITC experiments.

	Site 1	**Site 2**	**Site 3**	**Site 4**
K_a**(M^{-1})**	9.98E4 ± 8.6E2	9.77E4 ± 1.4E3	1.00E5 ± 2.7E3	1.02E5 ± 2.8E3
Δ*H* (cal·mol^{-1})	–187.7 ± 8.37	–159.4 ± 92.0	–353.1 ± 382	–470.0 ± 728
Δ*S* (cal·mol^{-1}·deg^{-1})	22.2	22.3	21.7	24.5

11. References

1. P. Y. Apel, Y. E. Korchev, Z. Siwy, R. Spohr and M. Yoshida, *Nuclear Instruments and Methods in Physics Research Section B*, 2001, **184**, 337-346.
2. M. Ali, P. Ramirez, H. Q. Nguyen, S. Nasir, J. Cervera, S. Mafe and W. Ensinger, *ACS Nano*, 2012, **6**, 3631-3640.
3. (a) S. A. Miller, V. Y. Young and C. R. Martin, *J. Am. Chem. Soc.*, 2001, **123**, 12335-12342; (b) G. W. Bishop, M. M. Lopez, P. Ramiah Rajasekaran, X. Wu and C. R. Martin, *J. Phys. Chem. C*, 2015, **119**, 16633-16638; (c) P. Jin, H. Mukaibo, L. P. Horne, G. W. Bishop and C. R. Martin, *J. Am. Chem. Soc.*, 2010, **132**, 2118-2119.
4. (a) G. Lee, W. Lee, H. Lee, S. Woo Lee, D. Sung Yoon, K. Eom and T. Kwon, *Appl. Phys. Lett.*, 2012, **101**, 043703; (b) J. Park, S. Lee, K. Jang and S. Na, *Biosens. Bioelectron.*, 2014, **60**, 299-304.
5. J. Wei, G. Du, J. Guo, Y. Li, W. Liu, H. Yao, J. Zhao, R. Wu, H. Chen and A. Ponomarov, *Nucl. Instrum. Methods Phys. Res., Sect. B*, 2017, **404**, 219-223.
6. Q. Wen, D. Yan, F. Liu, M. Wang, Y. Ling, P. Wang, P. Kluth, D. Schauries, C. Trautmann, P. Apel, W. Guo, G. Xiao, J. Liu, J. Xue and Y. Wang, *Adv. Funct. Mater.*, 2016, **26**, 5796-5803.